Contrib Mineral Petrol (1993) 113:424–435

Contributions to Mineralogy and Petrology

The role of phosphorus in rhyolitic liquids as determined from the homogeneous iron redox equilibrium

Rosa Gwinn* and Paul C. Hess

Department of Geological Sciences, Brown University, Providence, RI 02912, USA

Received June 17, 1991/Accepted July 28, 1992

Abstract. The redox ratio of iron is used as an indicator of solution properties of silicate liquids in the system (SiO-Al_2O_3-K_2O-FeO-Fe_2O_3-P_2O_5). Glasses containing 80-85 mol% SiO_2 with 1 mol% Fe_2O_3 and compositions covering a range of K_2O/Al_2O_3 were synthesized at 1400 °C in air (fixed fO_2). Variations in the ratio $FeO/FeO_{1.5}$ resulting from the addition of P_2O_5 are used to determine the solution behavior of phosphorus and its interactions with other cations in the silicate melt. In 80 mol% SiO_2 peralkaline melts the redox ratio, expressed as $FeO/FeO_{1.5}$, is unchanged relative to the reference curve with the addition of 3 mol% P_2O_5. Yet, the iron redox ratio in the 85 mol% SiO_2 potassium aluminosilicate melts *is* decreased relative to phosphorus-free liquids even for small amounts of P_2O_5 (0.5 mol%). The redox ratio in peraluminous melts is decreased relative to phosphorus- free liquids at P_2O_5 concentrations of 3 mol%. In peraluminous liquids, complexing of both Fe^{+3}-O-P^{+5} and Al^{+3}-O-P^{+5} occur. The activity coefficient of Fe^{+3} is decreased because more ferric iron can be accommodated than in phosphorus-free liquids. In peralkaline melts, there is no evidence that P^{+5} is removing K^+ from either Al^{+3} or Fe^{+3} species. In charge-balanced melts with 3 mol% Fe_2O_3 and very high P_2O_5 concentrations, phosphorus removes K^+ from K-O-Fe^{+3} complexes resulting in a redox increase. P_2O_5 should be accommodated easily in peraluminous rhyolitic liquids and phosphate saturation may be suppressed relative to metaluminous rhyolites. In peralkaline melts, phosphate solubility may increase as a result of phosphorus complexing with alkalis. The complexing stoichiometry may be variable, however, and the relative influence of peralkalinity versus temperature on phosphate solubility in rhyolitic melts deserves greater attention.

Introduction

Phosphorus generally comprises less than a few weight percent of most magmas yet it greatly influences their homogeneous and heterogeneous equilibria. Phase equilibria studies show that addition of P_2O_5 to pure SiO_2 melt depresses the tridymite liquidus and depolymerizes the SiO_2 melt (Ryerson and Hess 1980; Levin et al. 1969). In melts which contain a network modifying cation (SiO_2-M_xO_y), however, the addition of phosphorus polymerizes the melt through the formation of P^{+5}-O-M bonds. Stripping network modifying cations from Si-O-M complexes results in the formation of more Si-O-Si bonds which is reflected by an expansion of the stability of minerals with greater SiO_2 polymerization (Ryerson 1985; Kushiro 1975). The addition of phosphorus also affects the partitioning behavior of cations between immiscible silicate melts (Ryerson and Hess 1978; Watson 1976; Visser and Koster van Groos 1979). P_2O_5 is strongly partitioned into basaltic liquids coexisting with granitic immiscible liquids where it is stabilized by the abundance of network-modifying cations in the less polymerized liquids. Moreover, the distribution coefficient for rare earth elements (REE) between basalt and granite immiscible liquids is increased from 4 to 15 upon the addition of P_2O_5 to the system (Ryerson and Hess 1978). This argues for complexing of REE with phosphate species in the immiscible basalt. These data, also strongly supported by spectroscopic studies (Nelson and Tallant 1984; Mysen et al. 1981; Gan and Hess 1992; Dupree et al. 1989), imply that phosphorus has a strong affinity for network-modifying cations in general and trivalent cations in particular.

Phosphorus heterogeneous equilibria are also significant because of the ubiquity of phosphate minerals in igneous rocks. Apatite ($Ca_5(PO_4)_3(F, OH)$) occurs in igneous rocks ranging from basalt to rhyolite (Watson 1979a), and the volatile-free whitlockite ($Ca_3(PO_4)_2$) occurs in lunar basalts and eucrite meteorites (e.g., Hess et al. 1990). The saturation of these and other phosphate minerals in igneous systems depends on a multitude of chemical parameters, especially the activity of CaO, among other components, and the prevailing fluorine,

* Currently at: Dames and Moore, Inc., 7101 Wisconsin Avenue, Bethesda MD 20814, USA
Correspondence to: P.C. Hess

chlorine and water fugacities. Phosphorus often behaves incompatibly so that it becomes progressively enriched with fractionation (e.g. London 1987; Ryerson and Hess 1980). As fractionation increases P_2O_5 concentrations, the presence of phosphorus may promote liquid immiscibility or result in saturation of a phosphate mineral. It is also likely that phosphorus will have some influence on how trace elements, particularly trivalent cations, partition between melts and coexisting phases (Ryerson and Hess 1978).

The goal of the present study is to determine the solution properties of phosphorus in synthetic peralkaline, peraluminous and subaluminous granite melts using the variations of the homogeneous iron redox equilibrium as a probe of melt characteristics. Ferrous and ferric iron are accommodated differently within a silicate melt; the iron redox ratio macroscopically records how the melt maintains local charge-balance. The homogeneous iron equilibrium is well understood for the phosphorus-free system (Gwinn and Hess 1989; Dickenson and Hess 1981; 1986a,b) and provides a reference in measuring how melt structure is perturbed as P_2O_5 is added to or substituted into the melt. The iron redox ratio reflects how the accommodation of P^{+5} in granitic melts changes across the peraluminous to peralkaline boundary and the relative affinity of phosphorus for K^+, Fe^{+3}, or Al^{+3} in these melts.

Experimental and analytical techniques

Experimental methods

Large batches (approximately 1.5 g) of oxide mixtures of reagent grade powdered SiO_2, Al_2O_3, K_2CO_3, and Fe_2O_3 were prepared in the manner described in Gwinn and Hess (1989). P_2O_5 was added to the powders as a 0.3M solution of H_3PO_4 using a standard buret with a tolerance of $\pm$ 0.05 ml. The resulting slurry was dried at 110 °C and ground with a mortar and pestle in ethanol until the mixture was homogeneous (approximately 1 hour).

Six end-member phosphorus-bearing mixtures were prepared, each with 1 mol% Fe_2O_3. The P_2O_5 in each of these six mixtures was substituted for an equimolar amount of $K_2O + Al_2O_3$ so as to preserve the SiO_2 and Fe_2O_3 molar concentration. One pair of end-members contained 81 mol% SiO_2 and 3 mol% P_2O_5 with $K_2O/(K_2O + Al_2O_3)$ (= K* molar) of 0.30 or 0.70. The second pair had 85 mol% SiO_2 and contained 0.5 mol% P_2O_5 with K* of 0.30 or 0.70. The final pair of end-member mixtures contained 85 mol% SiO_2, 3 mol% P_2O_5, and K* of 0.30 or 0.70. Aliquots from the large end-member batches of powder were mixed to make intermediate compositions along the P_2O_5 isopleths. Isopleth A contains 81 mol% SiO_2 and 3 mol% P_2O_5. Isopleth B contains 85 mol% SiO_2 and 0.5 mol% P_2O_5. Isopleth C contains 85 mol% SiO_2 and 3 mol% P_2O_5.

The effect of differing phosphorus concentration at fixed K* was also investigated. Therefore, in addition to isopleths A, B and C, glasses with 3 mol% Fe_2O_3 and 3 or 6 mol% P_2O_5 were made. These were prepared by diluting an original base mixture (81 mol% SiO_2, 3 mol% Fe_2O_3, and K* = 0.5) with the appropriate amount of H_3PO_4.

Additionally, powder batches with 85 mol% SiO_2, no phosphorus, and 1 mol% Fe_2O_3 were made at K* ratios of 0.38, 0.46 and 0.70. The first two were mixed to attain an intermediate K* in the peraluminous region. Comparisons will be made later to the phosphorus-free glasses with 80 mol% SiO_2 as reported in Dickenson and Hess (1981).

The powders were compressed into small pellets and decarbonated at about 900 °C for a minimum of 2 hours. Following sintering, the pellets were loaded in Pt capsules, covered with crimped Pt caps, suspended in a vertical Del-Tech furnace, and equilibrated at 1400 °C ($\pm$ 2 °C) for a total run time of 24 h. Grinding and mixing of intermediate glasses was used to homogenize the glass samples. After the first 3 h at 1400 °C, the sample was quenched in water and dried. The glass was removed from the capsule, reground under acetone into a fine powder, repacked into the same capsule and returned to 1400 °C. Regrinding was repeated at the 6- and 12-hour intervals.

Analytical methods

A polished thin section of a portion of each glass sample was analyzed by electron microprobe at the Keck Foundation supported Electron Microprobe Facility, Brown University. Natural volcanic glasses were used as standards for SiO_2, Al_2O_3, K_2O, and FeO. P_2O_5 was standardized using an internal laboratory standard containing SiO_2, Al_2O_3, K_2O, CaO and P_2O_5. Five microprobe analyses of each glass were averaged and the standard deviation is reported with the analyses.

Ferrous iron was analyzed by volumetric microtitration (Thornber et al. 1980). Ferric iron was then calculated from the total iron analyzed by the microprobe using mass balance:

$$(Fe_2O_3 = [FeO_{probe} - FeO_{titration}] \times 1.1113).$$

Two titrations were performed on each glass, making the calculation of a standard deviation unfeasible. Instead, these values were averaged and the error in analysis equivalent to $\pm$ 60% (i.e., nearly equivalent to one standard deviation) was estimated using the Student's t-method (Skoog and West 1982). An evaluation of the uncertainty in titrations was also made using laboratory standard material TRS138-9D2 (supplied by J.G. Schilling of the University of Rhode Island). Five samples of the standard titrated with each batch of unknowns yielded an average value of 7.67 $\pm$ 0.12 wt.% FeO (accepted value 7.75 wt.% FeO).

Establishing equilibrium

Although equilibration time varies as a function of temperature, redox state, and sample composition, twelve hours are sufficient for the iron redox ratio to equilibrate in complex silicate melts as well as in potassium aluminosilicate melts similar to those of this study (e.g., Dickenson and Hess 1986a; Fox et al. 1982; Thornber et al. 1980). The standard deviation (σ) of microprobe analysis is used as an indication of the homogeneity of the sample. Compositions of inhomogeneous glasses will have analytical standard deviations greater than can be attributed to microprobe counting error. In all of the glasses equilibrated for 24 hours, σ calculated from the microprobe analysis is less than or equal to the error attributable to counting statistics alone indicating that the glass is homogeneous within the analytical technique (Chase and Rabinowitz 1967).

Results

Compositions of the P_2O_5-free, 85 mol% SiO_2 glasses are presented in Table 1. The data for 78–80 mol% SiO_2 glasses (1400 °C) are in Dickenson and Hess (1981). Data for P_2O_5- bearing 81 mol% SiO_2 and 85 mol% SiO_2 glasses are given in Tables 2 and 3, respectively. Glasses with K* > 0.5 are peralkaline and those with K* < 0.5 are peraluminous.

The most peralkaline base mixture with K* = 0.70 produced glasses with K* of 0.64, reflecting the loss of K_2O from peralkaline melts at high temperatures. Loss of

K_2O has been observed in very peralkaline liquids of other experimental studies (Dickenson and Hess 1981; Dickinson and Hess 1985). Thus, microprobe analysis of the final glass is absolutely necessary and a wide beam must be used in analysis.

Table 1. Composition of experimental glasses containing 85 mol% SiO_2, 1 mol% Fe_2O_3 and no phosphorus

	85:1	85:3	85:2	85:4
Wt%				
SiO_2	77.52	76.36	76.27	76.82
K_2O	6.44	7.93	8.96	12.65
Al_2O_3	11.75	12.45	11.51	6.39
P_2O_5	0.00	0.00	0.00	0.00
FeO	1.27	1.24	0.93	0.48
Fe_2O_3	1.27	1.44	1.69	2.16
Total	98.25	99.42	99.36	98.49
FeO*	2.41	2.54	2.45	2.42
mol%				
SiO_2	86.05	84.53	84.57	85.48
K_2O	4.56	5.60	6.34	8.98
Al_2O_3	7.69	8.12	7.52	4.19
P_2O_5	0.00	0.00	0.00	0.00
FeO	1.18	1.15	0.86	0.45
Fe_2O_3	0.53	0.60	0.70	0.90
K*	0.372	0.408	0.457	0.682
KF*	0.357	0.391	0.435	0.638
$\frac{FeO}{FeO_{1.5}}$	1.113	0.958	0.614	0.250

All analyses are by electron microprobe except ferrous and ferric iron. Ferrous iron is titrated and ferric iron is calculated by mass balance from total iron (FeO*) and titrated iron. K* is equal to $K_2O/(K_2O + Al_2O_3)$ on a mole basis. KF* is equal to $K_2O/(K_2O + Al_2O_3 + Fe_2O_3)$ in moles

The iron redox ratio expressed as $FeO/FeO_{1.5}$ (molar) is plotted as a function of K* in Fig. 1a for the 81 mol% SiO_2 glasses and in Fig. 1b for the 85 mol% SiO_2 glasses. The redox ratio for liquids containing no phosphorus, 78–80 mol% SiO_2 and 1 mol% Fe_2O_3 (1400 °C) are represented by a solid curve in Fig. 1a and b. This reference curve is a cubic polynomial fit to the data in the phosphorus-free system (Dickenson and Hess 1981). In Fig. 1b redox data for the P_2O_5-free 85 mol% SiO_2 glass are given by + symbols. Higher SiO_2 concentrations result in higher $FeO/FeO_{1.5}$ (see also Paul and Douglas 1965). The redox ratio at K* = 0.40 increases from 0.60 to about 0.80 and in peralkaline melts at K* = 0.68 the redox ratio increases from 0.17 to 0.26 with increasing SiO_2 contents.

In the peralkaline compositions (K* > 0.5) of glasses in isopleth A, the redox ratio is statistically unchanged from P_2O_5-free glasses and remains near 0.12 for all compositions (Fig. 1a, solid squares). Near K* = 0.55, however, the smoothed trend in $FeO/FeO_{1.5}$ increases virtually monotonically with decreasing K* but the redox ratio is less than in the P_2O_5-free glasses (solid curve). As glasses get more peraluminous, the difference between these two trends increases. For example, at K* = 0.45 the redox ratio is 0.35 in P_2O_5-free glasses but only 0.20 in P_2O_5-bearing glasses.

The ratio $FeO/FeO_{1.5}$ in glasses of isopleths B and C are plotted against K* in Fig. 1b (open circles and filled circles, respectively). Isopleth B (0.5 mol% P_2O_5) falls below the 85 mol% silica curve in both the peraluminous and peralkaline region, with redox ratios nearly identical to the reference curve for 78–80 mol% SiO_2. Isopleth C (3 mol% P_2O_5) is nearly identical to isopleth A in the peralkaline region but falls below isopleth A in the peraluminous region. In summary, the ratio $FeO/FeO_{1.5}$ is lowered by the addition of phosphorus in peraluminous

Table 2. Composition of experimental glasses of isopleth A containing 3 mol% P_2O_5 and 81 mol% SiO_2

	FP6	FP8	FP12	FP9	FP10	FP13	FP7
Wt.%							
SiO_2	69.78	69.45	69.21	69.58	70.06	70.02	70.47
K_2O	5.47	6.79	7.01	8.58	10.40	11.20	11.79
Al_2O_3	14.39	12.66	12.79	11.60	8.90	8.51	7.30
P_2O_5	6.47	6.84	6.73	7.19	7.17	6.96	6.86
FeO	0.80	0.61	0.60	0.42	0.25	0.21	0.25
Fe_2O_3	1.78	1.72	1.83	1.88	2.11	2.21	2.20
Total	98.69	98.07	98.17	99.25	98.89	99.11	98.87
FeO*	2.40	2.16	2.25	2.11	2.15	2.20	2.23
mol%							
SiO_2	81.30	81.42	81.17	80.92	81.49	81.29	81.72
K_2O	4.07	5.08	5.24	6.36	7.72	8.29	8.72
Al_2O_3	9.88	8.75	8.84	7.95	6.10	5.82	4.99
P_2O_5	3.19	3.39	3.34	3.54	3.53	3.42	3.37
FeO	0.78	0.60	0.59	0.41	0.24	0.20	0.24
Fe_2O_3	0.78	0.76	0.81	0.82	0.92	0.97	0.96
K*	0.292	0.367	0.372	0.445	0.558	0.588	0.636
KF*	0.276	0.348	0.352	0.420	0.523	0.550	0.594
$\frac{FeO}{FeO_{1.5}}$	0.500	0.395	0.364	0.250	0.130	0.103	0.125

All analyses are by electron microprobe except ferrous iron. Ferrous iron is titrated and ferric iron is calculated by mass balance. K* and KF* are as defined in Table 1 and the text

Table 3a. Composition of experimental glasses containing 0.5 mol% P_2O_5 and 85 mol% SiO_2

	FP1	FP11	FP3	FP4	FP5	FP2
Wt.%						
SiO_2	76.04	75.28	76.54	77.44	77.45	78.70
K_2O	6.55	7.68	8.15	9.27	9.71	10.91
Al_2O_3	12.27	12.36	11.11	9.78	8.39	6.54
P_2O_5	1.04	1.27	1.01	1.01	1.04	0.98
FeO	1.20	0.79	0.71	0.37	0.26	0.23
Fe_2O_3	1.42	1.58	1.66	2.01	2.36	2.47
Total	98.52	98.96	99.18	99.88	99.21	99.83
FeO*	2.48	2.21	2.20	2.18	2.38	2.45
mol%						
SiO_2	85.03	84.34	85.11	85.46	85.93	86.44
K_2O	4.67	5.49	5.78	6.53	6.87	7.64
Al_2O_3	8.09	8.16	7.28	6.36	5.49	4.23
P_2O_5	0.49	0.60	0.48	0.47	0.49	0.46
FeO	1.12	0.74	0.66	0.34	0.24	0.21
Fe_2O_3	0.60	0.67	0.69	0.84	0.98	1.02
K*	0.366	0.402	0.443	0.507	0.556	0.644
KF*	0.350	0.383	0.420	0.476	0.515	0.593
$\frac{FeO}{FeO_{1.5}}$	0.933	0.552	0.478	0.202	0.122	0.104

All analyses are by electron microprobe except ferrous iron. Ferrous iron is titrated and ferric iron is calculated by mass balance. K* and KF* are as defined in Table 1 and in the text

Table 3b. Composition of experimental glasses of isopleth C containing 3 mol% P_2O_5 and 85 mol% SiO_2

	FP20	FP22	FP23	FP15	FP21
Wt.%					
SiO_2	74.68	74.31	75.68	75.82	75.22
K_2O	4.43	5.37	6.32	7.35	10.23
Al_2O_3	11.69	11.30	9.58	6.38	5.52
P_2O_5	5.54	4.98	5.11	5.57	5.57
FeO	0.96	0.86	0.85	0.21	0.24
Fe_2O_3	1.64	1.76	1.98	2.47	2.38
Total	98.94	98.58	99.52	97.80	99.16
FeO*	2.44	2.44	2.63	2.43	2.38
mol%					
SiO_2	84.71	84.56	85.06	86.42	85.04
K_2O	3.21	3.90	4.53	5.34	7.38
Al_2O_3	7.81	7.58	6.35	4.29	3.68
P_2O_5	2.66	2.40	2.43	2.69	2.67
FeO	0.91	0.82	0.80	0.20	0.23
Fe_2O_3	0.70	0.75	0.84	1.06	1.01
K*	0.291	0.340	0.416	0.555	0.667
KF*	0.274	0.319	0.387	0.500	0.611
$\frac{FeO}{FeO_{1.5}}$	0.650	0.546	0.476	0.094	0.114

All analyses are by electron microprobe except ferrous iron. Ferrous iron is titrated and ferric iron is calculated by mass balance from total iron (FeO*)

Table 4. Composition of experimental glasses (wt.%) with P_2O_5 added as a dilutant

	FP18	FP19
Wt.%		
SiO_2	62.69	67.14
K_2O	10.94	11.39
Al_2O_3	9.21	9.59
P_2O_5	11.93	5.92
FeO	0.70	0.41
Fe_2O_3	3.30	3.88
Total	98.77	98.33
FeO*	3.67	3.90
mol%		
SiO_2	76.83	79.58
K_2O	8.55	8.61
Al_2O_3	6.65	6.70
P_2O_5	6.19	2.97
FeO	0.72	0.41
Fe_2O_3	1.52	1.73
K*	0.562	0.562
KF*	0.511	0.505
$\frac{FeO}{FeO_{1.5}}$	0.237	0.118

All analyses are by microprobe except ferrous iron. Ferrous iron is titrated and ferric iron is calculated by mass balance from FeO* (microprobe analysis of total iron) and FeO from titration

melts, shows no significant change in peralkaline melts with 81 mol% SiO_2, but is lowered in the 85 mol% SiO_2 peralkaline melts.

Two additional compositions were prepared by adding 3 and 6 mol% P_2O_5 as an H_3PO_4 dilutant to base mixtures containing 3 mol% Fe_2O_3 (Table 4). Each composition has a K* of 0.562 and nominally 80 mol% SiO_2. Increasing total iron in this concentration range should have little effect on $FeO/FeO_{1.5}$ in a peralkaline or charge-balanced melt (Dickenson and Hess 1986a; Mysen and Virgo 1989). Experiment FP19 (solid diamond, Fig. 3) is used to test this. It has higher Fe_2O_3 than isopleth A, but still only 3 mol% P_2O_5 added as a dilutant. The redox ratio for FP19 is the same as in the

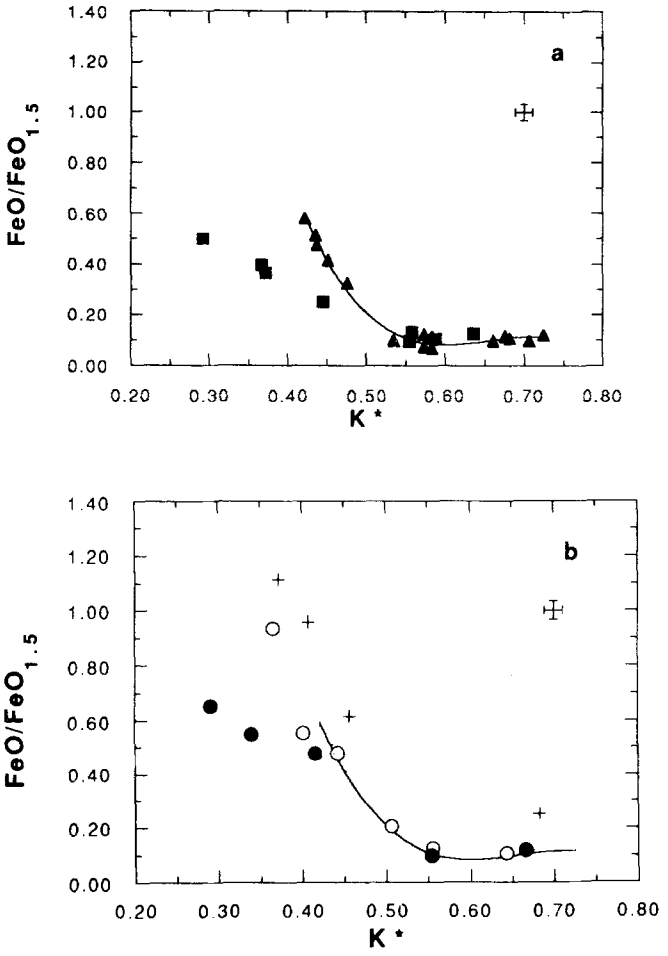

Fig. 1a, b. Iron redox ratio ($FeO/FeO_{1.5}$) as a function of K^* [$K_2O/[K_2O + Al_2O_3)$ molar] for experimental glasses equilibrated at 1400 °C in air. Average standard deviation from microprobe analysis is depicted by the error symbol. **a** Glasses with 81 mol% SiO_2, 1 mol% Fe_2O_3 and 3 mol% P_2O_5 are depicted by *filled squares*. Data for phosphorus free glasses with 78–80 mol% SiO_2 and 1 mol% Fe_2O_3 from Dickenson and Hess (1981) shown as *triangles*. The *solid curve* is a cubic polynomial fit to the phosphorus-free redox data of Dickenson and Hess (1981). **b** Glasses with 85 mol% SiO, 1 mol% Fe_2O_3 and 0.5 mol% P_2O_5 are depicted by *open circles*. Glasses with 85 mol% SiO_2, 1 mol% Fe_2O_3 and 3 mol% P_2O_5 are depicted by *filled circles*. Data for phosphorus-free redox equilibria and 78–80 mol% SiO_2 (Dickenson and Hess 1981) represented by the *solid curve*. Data for phosphorus free redox equilibria and 85 mol% SiO_2 from this study represented by the *plus signs*

3 mol% experiments of isopleth A. FP18, on the other hand, has twice as much P_2O_5 for the same amount of K^{ex}, and its redox ratio is *higher* than FP19.

In the P_2O_5-free glasses of Dickenson and Hess (1981), mullite ($3Al_2O_3.2SiO_2$) was encountered in peraluminous glasses with K^* less than about 0.42. In the present study, glasses with K^* as low as 0.29 did not crystallize mullite. The most peraluminous glasses (FP6, FP8, FP12 and FP20) saturated with tridymite, however. Because these experiments contain less than 1 vol % tridymite and the tridymite contains no iron, the glasses were titrated and included with the other data. Tridymite was never encountered in peralkaline liquids.

Discussion

Redox equilibrium and phosphorus-free melts

Understanding the solution properties of phosphorus in potassium aluminosilicate melts depends on our knowledge of the solution properties of P_2O_5-free melts. The properties of the base system (SiO_2-K_2O-Al_2O_3) are best understood by focusing on the effect of the ratio of alkalis to alkalis plus aluminum in these silicate melts (quantitatively described by K^* in the current study). A melt with $K^* = 0.5$ is formally charge-balanced with exactly enough K^+ to satisfy the charge-balancing requirements of tetrahedrally coordinated Al^{+3}. Melts with $K^* > 0.5$ are peralkaline and contain more K^+ than is needed to satisfy the needs of tetrahedral aluminum. This excess potassium (K^{ex}) can be used to stabilize other highly charged cations, such as for tetrahedral Fe^{+3}, Ti^{+4}, or Zr^{+4} (Hess 1991; Dickenson and Hess 1986a; 1985; Watson 1979b). The enhanced solubility of high field strength cations in peralkaline liquids is called the *peralkaline effect*.

Melts with $K^* < 0.5$ are peraluminous, i.e., contain Al^{+3} in excess of available charge-balancing K^+. This excess aluminum may be stabilized in triclusters or, in very peraluminous melts, may occur as five-, or six-coordinated aluminum (Risbud et al. 1987; Dickenson and Hess 1986a; Lacy 1963). Tetrahedral aluminum and its effort to gain the ideal charge-balancing stoichiometry dominates the solution properties in high-SiO_2 silicate melts.

The iron redox ratio is sensitive to the charge-balancing demands of aluminum. The homogeneous iron redox equilibrium is governed by the reaction:

$$FeO + \frac{1}{4}O_2 = FeO_{1.5} \quad (1)$$

The equilibrium constant for this reaction is

$$K_{eq} = \frac{a FeO_{1.5}}{a FeO} \cdot (f_{O_2})^{1/4} \quad (2)$$

where a FeO, and a $FeO_{1.5}$ are the appropriate activities and f_{O_2} is oxygen fugacity. K_{eq} is constant at constant T and P and f_{O_2} is fixed by air so the activity ratio of ferric to ferrous iron is a constant. Expressing the activity of a component as the product of the activity coefficient and the mole fraction of that component ($a = \gamma X$), and rearranging Eq. (2):

$$\frac{X FeO}{X FeO_{1.5}} = \frac{\gamma FeO_{1.5}}{\gamma FeO} \cdot \text{constant}(T, P, f_{O_2}) \quad (3)$$

According to Eq. (3), any variations in the ratio of ferrous to ferric iron are indicative of the inverse change in the ratio of their activity coefficients.

Spectroscopic and phase equilibrium studies have shown that ferric iron, like Al^{+3}, occurs predominantly in tetrahedral coordination in silicate melts and with alkalis as charge-balancing cations (Mysen and Virgo 1989; Brown et al. 1988; Dyar 1985; Dickenson and Hess 1981). In $KFeSi_3O_8$ and $Na(Al_{0-0.15}, Fe_{1-0.85})Si_2O_6$ glasses,

spectra analyzed with X-ray absorption near edge structure (XANES) and extended X-ray absorption fine structure (EXAFS) are consistent with tetrahedral ferric iron (Brown et al. 1988). Iron Mössbauer spectra of sodium aluminosilicate glasses are also consistent with tetrahedrally coordinated ferric iron in glasses with $FeO/FeO_{1.5} < 2$. Only as glasses become increasingly reduced ($FeO/FeO_{1.5} > 2$) do the Mössbauer data suggest a gradual shift to octahedrally coordinated ferric iron (Mysen and Virgo 1989).

Ferrous iron cannot be unequivocally assigned to either a formal octahedral or tetrahedral coordination in oxidized glasses. Infrared absorption combined with Raman spectroscopy of iron-bearing sodium silicate glasses indicates only octahedral ferrous iron (Fox et al. 1982). However, combined EXAFS and Mössbauer spectroscopy of iron alkali silicate glasses indicates that ferrous iron occurs in tetrahedral coordination (Waychunas et al. 1988).

In peralkaline melts, K^{ex} is available and the redox equilibrium favors the formation of ferric iron (Dickenson and Hess 1981). The result is a relatively low redox ratio reflecting the low $\gamma FeO_{1.5}/\gamma FeO$ (Fig. 1a, solid curve). In peraluminous liquids, however, there is insufficient K^+ to charge-balance Al^{+3} much less Fe^{+3}. As a result, the redox ratio rises sharply in peraluminous liquids relative to a charge-balanced liquid. This increase in $FeO/FeO_{1.5}$ reflects the decreased stability of ferric iron relative to ferrous iron in these melts, i.e. an increase in $\gamma FeO_{1.5}/\gamma FeO$ (Fig. 1a, solid curve).

The increase in redox ratio does not occur exactly at $K^* = 0.5$ in the system described already. Instead, the redox ratio begins to increase just before the melts become peraluminous, at approximately $K^* = 0.55$, and reflects the association of tetrahedrally coordinated aluminum and ferric iron with the charge-balancing cation K. To more adequately describe the charge-balancing capacity of the liquid we use the parameter $KF^* = K_2O/(K_2O + Al_2O_3 + Fe_2O_3)$. Recasting the redox ratio as a function of KF* (Fig. 2a, solid curve) illustrates that the increase in redox ratio occurs quite near $KF^* = 0.5$.

Finally, silica concentration affects $FeO/FeO_{1.5}$. Paul and Douglas (1965) have shown that in the SiO_2-K_2O system iron is increasingly reduced as the silica contents of glasses are increased, presumably due to a reaction like:

$$2KFe^{+3}O_2 + 6SiO_2 = 2Fe^{+2}Si_2O_5 + K_2Si_2O_5 + 1/2O_2 \quad (4)$$

where the state of polymerization of the silicate species on the right side of the equation are functions of the total K/Si ratio. Iron reduction is most significant at SiO_2 contents of 80 mol% and greater. Specifically, from 80 to 85 mol% SiO_2 in the SiO_2-K_2O system, $FeO/FeO_{1.5}$ increases from 0.20 to 0.40 (Paul and Douglas 1965).

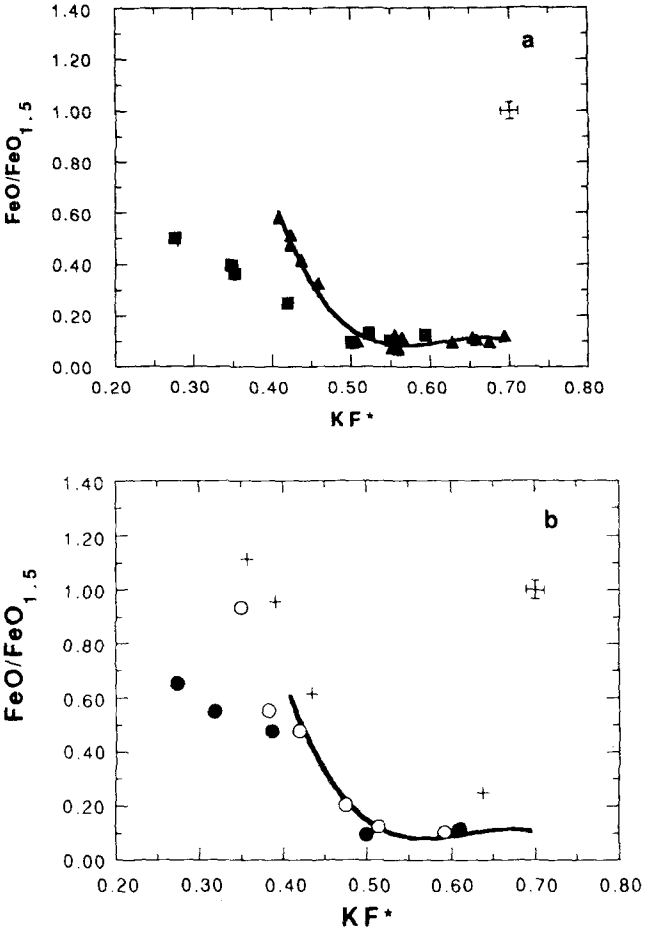

Fig. 2a, b. Iron redox ratio versus $KF^*[K_2O/(K_2O + Al_2O_3 + Fe_2O_3)]$ molar for glasses equilibrated at 1400 °C in air. **a** 81 mol% SiO_2 data. Symbols as in Fig. 1a; **b** 85 mol% SiO_2 data. Symbols as in Fig. 1b

Phosphorus in silicate melts

Phosphorus solution behavior in silicate melts has previously been investigated using both phase equilibria (Ryerson 1985; Ryerson and Hess 1980; Visser and Koster van Gross 1979) and spectroscopy (Gan and Hess 1992; Dupree et al. 1989, 1988a, b; Lu et al. 1988; Tallant and Nelson 1986; Nelson and Tallant 1984; Mysen et al. 1981). Phosphorus forms copolymerizing PO_4^{-3} tetrahedra in both peralkaline and peraluminous silicate melts. P-O-M complexes (where M = metal cation) are formed via the generalized reaction:

$$2Si\text{-}O\text{-}M + P\text{-}O\text{-}P = Si\text{-}O\text{-}Si + 2P\text{-}O\text{-}M \quad (5)$$

resulting in increased polymerization of the silicate network and an increase in γSiO_2 (e.g., Ryerson and Hess 1980).

The system SiO_2-Al_2O_3-K_2O-P_2O_5 has been investigated using ^{31}P MAS NMR and Raman spectroscopy (Gan and Hess 1992). In peralkaline melts, Gan and Hess (1992) determined that phosphorus combines with excess K^+ and forms K-O-P complexes as expressed by the reaction:

$$2Si\text{-}O\text{-}K + P\text{-}O\text{-}P = Si\text{-}O\text{-}Si + 2P\text{-}O\text{-}K \quad (6)$$

K_3PO_4 species predominate at low P_2O_5 concentrations but $K_4P_2O_7$ dimers and larger chains appear as P_2O_5 content of the melts increases. Simultaneous with the growth of potassium phosphate bands in the Raman

spectra, the low frequency bands (450–490 cm^{-1}) corresponding to increased Si-O-Si polymerization intensify as the reaction in Eq. (6) proceeds more completely to the right. Use of ^{31}P magic angle spinning NMR spectroscopy in Li_2O, Na_2O and K_2O silicate melts also shows that phosphorus combines with network-modifying alkalis to form orthophosphate and pyrophosphate species (Dupree et al. 1988a).

In peraluminous melts, phosphorus combines with excess Al^{+3} to form $AlPO_4$ complexes (Gan and Hess 1992) via the homogeneous equilibrium:

$$2\text{Al-O-Si} + \text{P-O-P} = 2\text{Al-O-P} + \text{Si-O-Si} \quad (7)$$

This reaction, like that in Eq. (6), requires that the activity coefficient of silica increase with phosphorus addition. Finally, Gan and Hess (1992) argue that in subaluminous glasses (i.e., $K_2O = Al_2O_3$) the incorporation of phosphorus is described by the reaction:

$$KAlO_2 + P_2O_5 = KPO_3 + AlPO_4 \quad (8)$$

in which aluminum-phosphate and potassium metaphosphate complexes are derived from the break-up of charged-balanced tetrahedral alumina.

Redox equilibria in phosphorus-bearing melts

Al^{+3}-O-P^{+5} and K^+-O-P^{+5} complexes are stable in peraluminous and peralkaline alkali aluminosilicate melts respectively. The iron redox equilibrium provides a sensitive probe to determine which solution mechanisms dominate in different composition melts and how iron interacts with these phosphate complexes.

Phosphorus has a strong affinity for trivalent aluminum and we may anticipate that the same will be true for phosphorus and Fe^{+3}. Mössbauer spectroscopy has been used to determine the coordination of iron in melts of the system P_2O_5-FeO-Fe_2O_3 and both ferrous and ferric iron are found in octahedral coordination (see Dyar 1985 for a summary of Mössbauer data). However, using other analytical techniques, tetrahedral ferric iron appears to predominate at low iron concentrations (i.e., less than 2 mol% Fe_2O_3). Two lines of evidence suggest that ferric iron will occur mostly in tetrahedral coordination in the melts of this study. First, by analogy, octahedrally coordinated Al^{+3} occurs only in glasses with the high concentrations of P_2O_5 (> 25 mol%) (Dupree et al. 1989), and octahedral coordination of ferric iron may likely be exclusive to high phosphorus systems. Indeed, tetrahedral ferric iron is found in CaO-Al_2O_3-SiO_2-FeO_x melts with up to 10 mol% P_2O_5 (Mysen 1990).

The results from this study also suggest that ferric iron is in tetrahedral coordination (i.e., behaving like Al^{+3}). A marked distinction in $FeO/FeO_{1.5}$ between peraluminous and peralkaline melts persists in P_2O_5-bearing systems (Fig. 1). As seen in the P_2O_5-free compositions, the decrease in $FeO/FeO_{1.5}$ occurs not where K^+ exactly balances Al^{+3} ($K^* = 0.5$) rather at higher K^* where $K^+ = (Al^{+3} + Fe^{+3})$. This dependence on both Al^{+3} and Fe^{+3} is illustrated in Fig. 2 where Fe^{+3} has been included in the charge-balanced expression $KF^* = K_2O/(K_2O + Al_2O_3 + Fe_2O_3)$. The shape of the redox curve suggests that the solution behavior in melts remains highly dependent on the formation of charge-balanced tetrahedral aluminum and ferric iron (Gwinn and Hess 1989; Dickenson and Hess 1986a).

The effect of phosphorus in the peraluminous region is to oxidize iron (Fig. 2a, b), i.e., the substitution of P_2O_5 for equimolar amounts of $K_2O + Al_2O_3$ has decreased the activity coefficient of ferric iron relative to ferrous iron. Furthermore, the *relative* oxidation of iron increases as KF^* decreases. In other words, more peraluminous melts witness a relatively greater stabilization of ferric iron with phosphorus substitution. A mechanism by which ferric iron is stabilized relative to ferrous iron in increasingly peraluminous melts is required.

Consider the homogeneous equilibrium for P_2O_5-free peraluminous melts

$$2KFe^{+3}O_2 + Al_2O_3 = 2KAl^{+3}O_2 + 2FeO + 1/2\ O_2 \quad (9)$$

which describes the reduction of iron with increasing excess aluminum (Al_2O_3). If upon the addition of P_2O_5 Al^{+3}-O-P^{+5} species form, Al^{ex} is removed from competition with Fe^{+3} for K^+, the effective peraluminosity of the liquids is reduced and Eq. (9) proceeds more to the left. From the studies of the P_2O_5-bearing iron-free system, we know that the occurrence of excess Al^{+3} as triclusters or in high coordination is less favorable than as $AlPO_4$ complexes (Gan and Hess 1992). The lack of tricluster aluminum in the iron- bearing liquids is also supported by the heterogeneous phase equilibria in the very peraluminous liquids of this study.

Dickenson and Hess (1981) encountered the mullite ($3Al_2O_3 \cdot 2SiO_2$) saturation surface in P_2O_5-free peraluminous melts with K^* less than about 0.42. In contrast, tridymite rather than mullite crystallized from the most peraluminous P_2O_5-bearing glasses of this study. This implies that the activity of SiO_2 has increased and the activity of Al_2O_3 has decreased upon substitution of P_2O_5 such that the equilibrium:

$$3Al_2O_3 \cdot 2SiO_2 + 3P_2O_5 = 6AlPO_4 + 2SiO_2 \quad (10)$$

is shifted to the right.

Another scenario to describe the iron redox equilibrium in peraluminous melts requires the increased stabilization of ferric iron directly by phosphorus. It is possible, if not likely, that Fe^{+3}-O-P^{+5} species analogous to aluminum phosphate species are generated. Given the many similarities in solution properties between Al^{+3} and Fe^{+3} this is quite reasonable. The effect of forming ferric phosphate species is to reduce $\gamma FeO_{1.5}$, occurring via the reaction

$$2Fe^{+2}O + P_2O_5 + 1/2O_2 = 2Fe^{+3}PO_4 \quad (11)$$

in which ferrous iron is oxidized to ferric iron in order to accommodate P^{+5} in $Fe^{+3}PO_4$ complexes. Moreover, as the nominal concentration of ferrous iron in the melts increases, the reaction in Eq. (11) proceeds more to the right and increases the iron oxidation. Such an effect is observed: the decrease in the redox ratio is greatest in the most peraluminous melts where the liquids initially contain more ferrous iron.

Specifically, at low concentration, phosphorus interacts with small amounts of Al_2O_3 and FeO such that the

effect on redox ratio in isopleth B (0.5 mol% P_2O_5) is intermediate to isopleth C (3 mol% P_2O_5) and the 85 mol% liquids in peraluminous melts (Fig. 2b). Moreover, the redox curves fan out with increased P_2O_5 concentrations. The fanning out may be explained by a competition between iron and aluminum for phosphorus. Initially, phosphorus and excess aluminum combine according reaction of Eq. (10), but as P_2O_5 increases, $Fe^{+3}PO_4$ becomes an increasingly important fraction of the phosphate complexes (Eq. 11).

The relative extent to which Eq. (10) and (11) occur in peraluminous melts is represented by the offset of the redox equilibrium curve. If only Al^{+3}-O-P complexes form (Eq. 10), then the effective Al^{ex} is diminished and the redox ratio would be decreased to reflect the 'effective' K*. Yet, in very peraluminous melts the amount of Al^{ex} remaining after satisfying P^{+5} is greater than that implied by the redox ratio. For example, in FP6 (K* equals 0.29) Al^{ex} is 5.81 moles. Aluminum in excess of both potassium and phosphorus is 2.62 moles. For the same total moles of $K_2O + Al_2O_3$, this translates to an effective K* of 0.41. The redox ratio at K* = 0.41 without P_2O_5 should be approximately 0.68. The actual redox ratio is 0.50, suggesting direct ferric iron stabilization (Eq. 11). Thus, a purely aluminum mechanism is inadequate in explaining the homogeneous iron redox adjustment.

If, however, only Fe^{+3}-O-P complexes formed (Eq. 11), the redox ratio would shift down for a given K* reflecting the increased stability of Fe^{+3}. In all P_2O_5-bearing melts, there is far more P^{+5} than needed to form the additional ferric iron and, therefore, the iron oxidation reaction alone cannot adequately describe the entire system. The relative extent to which Eqs. (10) and (11) describe the redox changes is adjusted throughout the peraluminous region.

The homogeneous equilibria in peralkaline melts are quite different from those in peraluminous ones. In 81 mol% SiO_2 glasses, $FeO/FeO_{1.5}$ in P_2O_5-bearing peralkaline melts are not significantly changed from those in melts without phosphorus (Fig. 2a). At 85 mol% SiO_2 the redox ratio in P_2O_5 glasses are lower than those in P_2O_5-free glasses. Two possible solution mechanisms for phosphorus are suggested. First, P^{+5} may complex with K^{ex}, as anticipated from NMR and Raman spectroscopy studies (Gan and Hess 1992). Recall that the extent of phosphate polymerization is controlled by the K^{ex}/P (Gan and Hess 1992). Complexing of phosphorus with excess potassium is described by the reaction:

$$2K\text{-}O\text{-}Si + P\text{-}O\text{-}P = 2K\text{-}O\text{-}P + Si\text{-}O\text{-}Si \quad (12)$$

in which only the network modifying K^{ex} is used by phosphorus. This reaction stabilizes phosphorus without necessarily disturbing the iron redox ratio in peralkaline melts.

In the second scenario, the redox ratio is lowered by the addition of phosphorus if Fe^{+3} and P^{+5} combine to form $Fe^{+3}PO_4$. As described by Eq. (11), ferrous iron is oxidized to form $Fe^{+3}PO_4$ species, and thereby decreases $FeO/FeO_{1.5}$. Such a decrease occurs in the peralkaline melts with 85 mol% SiO_2, in fact, to the point that the redox ratio is virtually identical to that in the 81 mol% SiO_2 glasses.

In phosphorus-free peralkaline melts, the redox ratio is nearly unaffected by increasing K*, suggesting that the maximum stabilization of ferric iron at these conditions is reached when excess potassium is available. In melts with 80 mol% SiO_2, the addition of P^{+5} may stabilize additional iron, but this minor increment is virtually unmeasurable. By increasing SiO_2 to 85 mol% and thereby increasing $FeO/FeO_{1.5}$, the stabilizing effect on ferric iron of adding P_2O_5 is more apparent in the homogeneous equilibria, and additional ferric iron is formed. However, a mere 0.10 mol% additional Fe_2O_3 forms, suggesting that only small amounts of phosphorus are interacting with the iron and most of the P^{+5} is accomodated by K^{ex}.

In charge-balanced melts, the competition between phosphorus, aluminum and ferric iron for K^{ex} is maximized. As in the peralkaline melts, stripping K^+ from ferric iron would increase the redox ratio. If Fe^{+3}-O-P^{+5} bonding occurred, ferric iron would become more stable and $FeO/FeO_{1.5}$ would decrease. Finally, if $AlPO_4$ formed, the released K could stabilize ferric iron in the melt. These possibilities can be tested in melts with minimal K^{ex}, i.e., with KF* near 0.5, and high concentrations of iron and phosphorus. Therefore, experiments with greater total Fe_2O_3 and P_2O_5 near KF* = 0.5 were performed to test these ideas (Table 4).

Experiments with 3 mol% Fe_2O_3 and either 3 or 6 mol% P_2O_5 at a charge-balanced composition are illustrated in Fig. 3. Higher P_2O_5 concentrations have greater $FeO/FeO_{1.5}$. These data support the hypothesis that K^+-O-P^{+5} species are formed in the charge-balanced liquids at the expense of $KFe^{+3}O_2$. The iron responds by reducing to Fe^{+2} in a reaction of the sort

$$2KFe^{+3}O_2 + P_2O_5 = 2KPO_3 + 2Fe^{+2}O + 1/2O_2 \quad (13)$$

It is clear, however, that only a small fraction of P_2O_5 is accomodated by this equilibrium since there is only a modest increase in $FeO/FeO_{1.5}$ even though

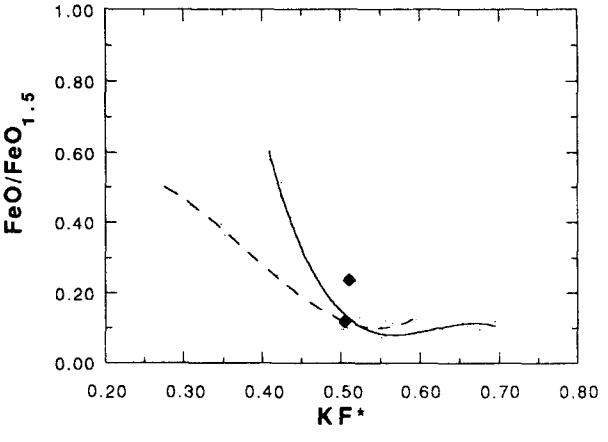

Fig. 3. Iron redox ratio versus KF*[$K_2O/(K_2O + Al_2O_3 + Fe_2O_3)$ molar] for glasses equilibrated at 1400 °C in air. *Diamonds* represent the redox ratio in nearly charge-balanced experiments with 3 mol% Fe_2O_3 and either 3 mol% P_2O_5 or 6 mol% P_2O_5. The *dashed curve* represents the redox ratio in the glasses of isopleth A (81 mol% SiO_2, 1 mol% Fe_2O_3 and 3 mol% P_2O_5). *Solid curve* represents the reference for phosphorus free glasses (Dickenson and Hess 1981)

$P_2O_5 \geq Fe_2O_3$. The solution of P_2O_5 in these nominally charge-balanced melts is described by Eq. (8), or by Eq. (14)

$$KAlO_2 + KPO_3 + 2FeO + 1/2O_2 = 2KFe^{+3}O_2 + AlPO_4 \quad (14)$$

which is obtained by combining Eq. 8 and 13. Since most of the total iron exists as Fe^{+3} it follows that most of the P is accomodated as $AlPO_4$ species. Thus the right hand side of the reaction is greatly favored in these melts.

Applying the model to additional data

Dickenson (1984) also performed experiments on phosphorus in this system. The differences between those data and the current study are manifold. Dickenson's experiments were performed at 1450 °C for a minimum of 16 h on nominally 78 mol% SiO_2 glasses with 1 mol% Fe_2O_3, and 5 mol% P_2O_5. P_2O_5 was substituted for a molar equivalent of $K_2O + Al_2O_3$ although SiO_2 ranges from 75 to 82 mol% in the final glasses.

The redox ratio versus K* at 1450 °C is illustrated in Fig. 4a. The redox ratio in peraluminous liquids with 5 mol% P_2O_5 is not as oxidized as in the present study (Fig. 4a) and in the peralkaline liquids is greater than the base system. However, increasing temperature causes the redox reaction in Eq. (1) to proceed more to the left, i.e, to reduce iron. Therefore, to enable comparison the data must be adjusted for temperature. Temperature calibrations in iron-bearing redox systems have been performed by Sack et al. (1981) and refined by Kilinc et al. (1983). Using the temperature coefficients from these studies the 1450 °C data have been recalculated to 1400 °C.

Figure 4b includes the temperature-corrected data with 5 mol% P_2O_5 with nominally 78 mol% SiO_2 and the data from isopleth A (3 mol% P_2O_5 and 81 mol% SiO_2). The corrected redox ratio is nearly identical with that of isopleth A of this study suggesting that the effect beyond 3 mol% P_2O_5 is minimal in the silicate melts.

Dickenson's temperature corrected data substantiate our model for peralkaline melts. The uniformity of peraluminous redox ratios for 3 and 5 mol% P_2O_5 concentrations, however, must be addressed. These melts all have P_2O_5 substituted for a peraluminous ($K_2O + Al_2O_3$) component of a base melt. Therefore, the *relative* amount of excess aluminum in peraluminous melts is less for the compositions with higher phosphorus concentration. It follows, therefore, that the Al-tricluster concentration is reduced whereas the P_2O_5 concentration is increased. The net effect on the homogeneous equilibria (Eq. 10) are nearly balanced and major effects on the iron redox equilibrium are not observed.

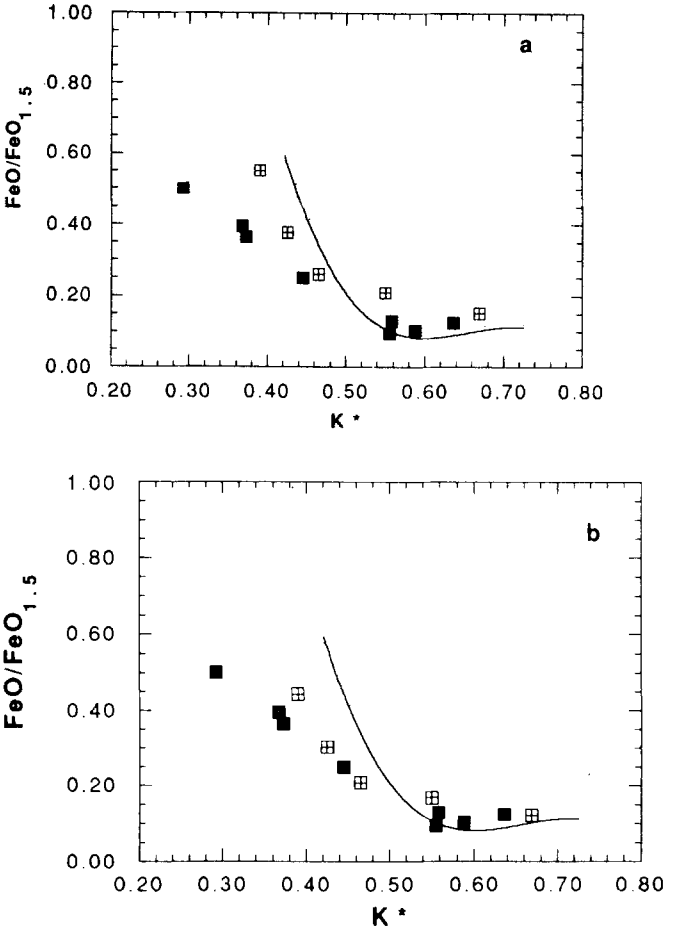

Fig. 4. a Iron redox ratio versus K* for glasses of isopleth A (*solid squares*), and those with 5 mol% P_2O_5 at 1450 °C (Dickenson 1983) (*boxes*), and the 78–80 mol% SiO_2 *reference curve* (Dickenson and Hess 1981). **b** Iron redox ratio versus K* for glasses of isopleth A (*solid squares*), and the temperature-corrected data with 5 mol% P_2O_5 (Dickenson 1984) (*boxes*), and the 78–80 mol% SiO_2 *reference curve* (Dickenson and Hess 1981)

Phosphate solubilities in metaluminous and peralkaline silicate melts

The solubility of the phosphate minerals in silicate melts is controlled by temperature, pressure and composition. From the present study it is suggested that phosphate solubility may be increased by extreme peraluminosity and peralkalinity (measured by the agpaitic index (AI $= (Na_2O + K_2O) / Al_2O_3$)) at constant temperature and SiO_2 concentrations. The solubility of apatite decreases as liquid SiO_2 content increases and temperature decreases and, as a result, is relatively low in granitic rocks (Harrison and Watson 1984; Green and Watson 1982). The silica dependence, however, is more correctly ascribed to the decreased availability of network modifiers to phosphorus as silica contents increase.

Temperatures in peralkaline, metaluminous and peraluminous rhyolites differ considerably. In the system SiO_2-Al_2O_3- Na_2O-K_2O-H_2O, liquidus temperatures in peraluminous silicate melts are somewhat higher than peralkaline ones (Holz et al. 1992; Gwinn 1991; Levin et al. 1969). Based on temperature considerations alone, the solubility of phosphate should be greatest in peraluminous granitic melts barring other moderating factors. Moreover, it is suggested that phosphate solubility is enhanced in peraluminous liquids by the peraluminous effect. The Macusani rhyolite, for example, is a strongly

peraluminous rhyolite obsidian with AI = 0.68 and a P_2O_5 concentration of 0.55 wt.% (Pichavant et al. 1987). Even more elevated P_2O_5 contents are observed in some peraluminous granites (~1 wt.%) (London 1992; Pichavant and Montel 1988), although these may not all be phosphorus contents of liquids. Apatite saturated metaluminous rhyolites, in contrast, typically contain less than 0.10 wt% P_2O_5 (e.g. Hildreth 1979).

The high solubility of phosphate in the Macusani liquids is not solely an expression of the peraluminous effect as other peraluminous granites, albeit with higher AI (i.e., less peraluminous), have lower P_2O_5 contents (0.10–0.20 wt.%; White and Chappell 1988). A notable feature of the Macusani rhyolite is the high boron concentration, 0.62 wt.% B_2O_3 (Pichavant et al. 1987). Given the B^{+3}-Al^{+3} diadochy in the quartz-like structure of (B^{+3}, Al^{+3}) PO_4 (Wells 1984), boron and aluminum are likely to behave similarly in silicate melts although recent spectroscopic results (Gan et al. 1992) suggest that these relations are complex. The high boron content is expected to further stabilize phosphorus in the melts and increase phosphate solubility. Similar occurrences are recorded in boron-rich pegmatities (London 1987).

By the same token, phosphate solubility should be enhanced by peralkalinity and this has been verified experimentally for the mineral monazite (REE-PO_4) (Ellison and Hess 1988; Montel 1986). Specifically, the solubility of lanthanum monazite ($LaPO_4$) increases by a factor of four over the range of AI = 1.00 to AI = 1.50 in the base system SiO_2-Al_2O_3-K_2O (Ellison and Hess 1988). However, increasing peralkalinity in a suite of peralkaline rhyolites commonly indicates fractionation and a concomitant decrease in temperature. Thus, the predicted four-fold increase in phosphate solubility might be entirely offset by a temperature decrease from, for example, 850 °C to 750 °C in a granitic system (Harrison and Watson 1984).

Peralkaline rhyolites can be produced by fractionation of plagioclase feldspar from trachytic magmas (Bowen 1945). Subsequent rhyolites evolve to higher AI as alkali feldspar fractionates from the magmas (e.g., Nicholls and Carmichael 1969). Thus, increasing AI is accompanied by reduced temperatures in magmatic systems. Although reliable temperature estimates are made difficult by the paucity of Fe-Ti oxides in peralkaline rhyolites, experimental evidence indicates that agpaitic indices as high as 1.6 can be produced by fractionation of a rhyolite with AI = 1.3 from the 750 °C – 600 °C interval (Gwinn 1991). Thus, depending on the particular fractionating system, temperature can drop from ~900 °C in trachytes (e.g., Johnson 1990) to ~700 °C or less in peralkaline rhyolites.

One example of a well-characterized trachyte-pantellerite suite is the Boina sequence, Ethiopia (Barberi et al. 1975). P_2O_5 concentration reaches a maximum of 0.72 wt.% in the trachytic rocks of Boina and decreases to as low as 0.01 wt.% in the rhyolitic stage, despite an increase in agpaitic index to 1.58! Decreasing phosphorus must be due to the continued fractionation of a phosphate, yet P_2O_5 contents are significantly less than the predicted saturation level (approximately 0.14 wt.% P_2O_5 at ~800 °C in a peralkaline experiment; Watson and Capobianco 1981). Applying experimentally-determined thermal- and silica-dependent constraints from the more extensive results of Harrison and Watson (1984), the decrease in phosphorus saturation levels from trachyte to peralkaline rhyolite correspond to a temperature drop from approximately 925 ° in the trachyte to 750 °C in the rhyolite. These temperatures are entirely consistent with a fractionation model. Thus, despite increasing peralkalinity, the fractionating rhyolitic melt remains phosphate saturated presumably due to temperature effects. These conclusions appear to apply generally since the concentration of P_2O_5 is very low, often less than 0.10 wt.% in glasses, and does not increase with increased peralkalinity in cogenetic peralkaline suites (e.g., Macdonald et al. 1987; Civetta et al. 1984; Bizouard et al. 1980). Clearly the peralkaline effect is masked by temperature.

Finally, solution properties suggest that charge-balanced melts have the lowest phosphate solubilities. In nature, these melts are most closely approximated by the metaluminous granites and rhyolites, i.e., those for which ($CaO + K_2O + Na_2O$) > Al_2O_3 > ($K_2O + Na_2O$). The metaluminous 'early rhyolite' of the Latir volcanic field, for example, contains apatite phenocrysts, yet the whole-rock analyses yield only 0.08–0.05 wt.% P_2O_5 (Johnson and Lipman 1988). In addition, apatite occurs as inclusions in other phenocrysts in the Bishop Tuff rhyolites (0.01–0.06 wt.% P_2O_5, whole rock), implying that it saturated relatively early in the crystallization sequence (Hildreth 1979) although the possibility of local saturation due to crystal-liquid boundary-layer phenomena cannot be discounted.

Conclusions

The iron redox ratio has been used to investigate the relative stabilization mechanisms for P^{+5} in potassium aluminosilicate melts. These melts are a simplified analogue for the granite system containing both iron and phosphorus. In phosphorus-bearing peraluminous liquids the redox ratio of iron is decreased relative to phosphorus-free liquids, suggesting the formation of Al^{+3}-O-P^{+5} and Fe^{+3}-O-P^{+5} species in the form of $AlPO_4$ and $FePO_4$-type complexes. In peralkaline liquids, phosphorus is accommodated by forming a range of K-O-P complexes. For the most peralkaline melts, there is sufficient K^+ to form both Fe^{+3}-O-K^+ and P^{+5}-O-K^+ species. The most dramatic effects occur in subaluminous liquids in which there are no Al^{ex} or K^{ex} species to combine with P_2O_5. A small fraction of P_2O_5 combines with charge-balancing potassium associated with ferric tetrahedra causing a modest increase in the redox ratio. Most of the P_2O_5, however, is dissolved as $AlPO_4$ and KPO_3 complexes, as indeed occurs in Fe-free melts.

The presence of excess alkalis or excess aluminum in granitic liquids should strongly influence the formation of phosphate minerals. The relative impact of the peralkaline and peraluminous effect on the solubility of phosphates is governed by many competing factors in natural systems including source region, temperature, and alkali earth concentrations. The ubiquitous occurrence of phosphates combined with the dominant role these minerals

play in the REE budgets of rocks suggest that phosphate saturation and phenocryst/melt pairs in a compositional range including peraluminous and peralkaline granites over a range of temperatures is warranted.

Acknowledgements. The work presented in this paper was performed under the support of NSF Grant 8719358. The manuscript was greatly improved by thoughtful and thorough reviews by Dr. Victor C. Kress and Dr. E. Bruce Watson.

References

Barberi F, Ferrara G, Santacroce R, Treuil M, Varet J (1975) A transitional basalt-pantellerite sequence of fractional crystallization, the Boina centre (Afar rift, Ethiopia). J Petrol 16:22–56

Bizouard H, Barberi F, Varet J (1980) Mineralogy and petrology of Erta Ale and Boina volcanic series, Afar rift, Ethiopia. J Petrol 21:401–436

Bowen NL (1945) Phase equilibria bearing on the origin and differentiation of the alkaline rocks. Am J Sci 243A:75–89

Brown GE Jr, Calas G, Waychunas GA, Petiau J (1988) X-ray absorption spectroscopy and its applications in mineralogy and geochemistry. In: Hawthorne FC (ed) Spectroscopic methods in mineralogy and geology. Reviews in Mineralogy 18:431–512

Chase GD, Rabinowitz JL (1967) Principles of radioisotope methodology (3rd edn.) Burgess Publ Co, Minneapolis MN, pp 75–108

Civetta L, Cornette Y, Crisci G, Gillot PY, Orsi G, Requejo CS (1984) Geology, geochronology and chemical evolution of the island of Pantelleria. Geol Mag 121:541–668

Dickenson MP (1984) The structural role and homogeneous redox equilibria of iron in peraluminous, metaluminous, and peralkaline silicate melts. PhD Thesis Brown University, Providence, USA

Dickenson MP, Hess PC (1986a) The structural role and homogeneous redox equilibria of iron in peraluminous, metaluminous and peralkaline silicate melts. Contrib Mineral Petrol 92: 207–217

Dickenson MP, Hess PC (1986b) The structural role of Fe^{3+}, Ga^{3+}, Al^{3+} and homogeneous iron redox equilibria in K_2O-Al_2O_3-Ga_2O_3-SiO_2-Fe_2O_3-FeO melts. J Non-Cryst Solids 86:303–310

Dickenson MP, Hess PC (1981) Redox equilibria and the structural role of iron in alumino-silicate melts. Contrib Mineral Petrol 78:352–357

Dickinson JE, Hess PC (1985) Rutile solubility and titanium coordination in silicate melts. Geochim Cosmochim Acta 49: 2289–2296

Dupree R, Holland D, Mortuza MG, Collins JA, Lockyer MWG (1989) Magic-angle spinning NMR of alkali phospho-aluminosilicate glasses. J Non-Crystal Solids 112:111–119

Dupree R, Holland D, Mortuza MG (1988a) The role of small amounts of P_2O_5 in the structure of alkali disilicate glasses. Phys Chem Glasses 29:18–21

Dupree R, Holland D, Mortuza MG, Collins JA, Lockyer MWG (1988b) An MAS NMR study of network-cation coordination in phosphosilicate glasses. J Non-Crystal Solids 106:403–407

Dyar MD (1985) A review of Mössbauer data on inorganic glasses: the effects of composition on iron valency and coordination. Am Mineral 70:304–316

Ellison AJG, Hess PC (1988) Peraluminous and peralkaline effects upon "monazite" solubility in high-silica liquids. EOS 69:498

Fox KE, Furukawa T, White WB (1982) Transition metal ions in silicate melts. Part 2. Iron in sodium silicate glasses. Phys Chem Glasses 23:169–178

Gan H, Hess PC (1992) Phosphorus speciation in potassium aluminosilicate melts. Am Mineral 177:501–512

Gan H, Hess PC, Kirkpatrick RJ (1992) Heirarchy of interactions between Si-B-K-P in granitic melts. EOS 73:357

Green TH, Watson EB (1982) Crystallization of apatite in natural magmas under high-pressure, hydrous conditions, with particular reference to "orogenic" rock series. Contrib Mineral Petrol 79:96–105

Gwinn RE (1991) The peralkaline effect in rhyolitic melts: iron titanium oxide solubility; Phosphorus solution properties and the iron redox equilibrium; phase equilibria in a peralkaline rhyolite. PhD Thesis, Brown University, Providence, USA

Gwinn R, Hess PC (1989) Iron and titanium solution properties in peraluminous and peralkaline rhyolitic liquids. Contrib Mineral Petrol 101:326–338

Harrison TM, Watson (1984) The behavior of apatite during crustal anatexis: equilibrium and kinetic considerations. Geochim Cosmochim Acta 48:1467–1477

Hess PC (1991) The role of high field strength cations in silicate melts. In: Advances in physical chemistry, vol. 9, Springer, New York Berlin Heidelberg, pp 152–191

Hess PC, Horzempa P, Rutherford MJ, Devine J (1990) Phosphate equilibria in lunar basalts. (Abstr) Lunar Planet Sci Conf XXI:505–506

Hildreth W (1979) The Bishop Tuff: evidence for the origin of compositional zonation in silicic magma chambers. Geol Soc Am Spec Pap 180:43–75

Holz F, Johannes W, Pichavant M (1992) Effect of excess aluminum on phase relations in the system Qz-Ab-Or: experimental investigation at 2 kbar and reduced H_2O activity. Eur J Mineral 4:137–152

Johnson MC (1990) Intensive parameters of volcanic magma systems from experimental amphibole/melt equilibria. PhD Thesis, Brown University, Providence, USA

Johnson CM, Lipman PW (1988) Origin of metaluminous and alkaline rocks of the Latir volcanic field, northern Rio Grande rift, New Mexico. Contrib Mineral Petrol 100:107–128

Kilinc A, Carmichael ISE, Rivers ML, Sack RO (1983) The ferric-ferrous ratio of natural silicate liquids equilibrated in air. Contrib Mineral Petrol 83:136–140

Kushiro I (1975) On the nature of silicate melts and its significance in magma genesis: regularities in the shift of liquidus boundaries involving olivine, pyroxene, and silica minerals. Am J Sci 275:411–431

Lacy ED (1963) Aluminum in glasses and in melts. Phys Chem Glasses 4:234–238

Levin EM, Robbins CR, McMurdie HF (1969) Phase diagrams for ceramists. 1969 Supplement. Am Ceram Soc Inc, Columbus Ohio

London D (1987) Internal differentiation of rare-element pegmatites: effects of boron, phosphorus, and fluorine. Geochim Cosmochim Acta 51:403–420

London D (1992) Phosphorus in S-type magmas: the P205 content of feldspars from peraluminous granites, pegmatites, and rhyolites. Am Mineral 77:126–145

Lu Y, Ding A, Tang Y (1988) Structural change of soda lime glass with minor P_2O_5 addition and heat treatment. J Non-Cryst Sol 106:391–394

Macdonald R, Davies GR, Bliss CM, Leat PT, Bailey DK, Smith RL (1987) Geochemistry of high-silica peralkaline rhyolites, Naivasha, Kenya Rift Valley. J Petrol 28:979–1008

Montel JM (1986) Experimental determination of the solubility of Ce-monazite in SiO_2-Al_2O_3-K_2O-Na_2O melts at 800°C, 2 kbar, under H_2O-saturated conditions. Geology 14:659–662

Mysen BO (1990) Interaction between phosphorous and iron oxides in silicate melts. Annual Report of the Director of the Geophysical Laboratory, Carnegie Instn Washington, 1989-1990, Geophysical Laboratory, Washington DC 66–75

Mysen BO, Virgo D (1989) Redox equilibria, structure, and properties of Fe-bearing aluminosilicate melts: relationships among temperature, composition, and oxygen fugacity in the system Na_2O-Al_2O_3-SiO_2-Fe-O. Am Mineral 74:58–76

Mysen BO, Ryerson FJ, Virgo D (1981) The structural role of phosphorus in silicate melts. Am Mineral 66:106-117

Nelson C, Tallant DR (1984) Raman studies of sodium silicate glasses with low phosphate contents. Phys Chem Glasses 25: 31–38

Nicholls J, Carmichael ISE (1969) Peralkaline acid liquids: a petrological study. Contrib Mineral Petrol 20:268–294

Paul A, Douglas RW (1965) Ferrous-ferric equilibrium in alkali silicate glasses. Phys Chem Glasses 6:207–211

Pichavant M, Montel JM (1988) Petrogenesis of a two-mica ignimbrite suite: the Macusani Volcanics, SE Peru. Trans Roy Soc Edinburgh: Earth Sci 73:197–207

Pichavant M, Verrara JV, Boulmet S, Brique L, Joron J-L, Juteau M, Marin L, Michard A, Sheppared SMF, Treuil M, Vernet M (1987) The Macusani glasses, SE Peru: evidence of chemical fractionation in peraluminous magmas. In: Mysen BO (ed) Magmatic processes: physicochemical principles. Geochem Soc Spec Publ 1:359–373

Risbud SH, Kirkpatrick RJ, Taglialavore AP, Montez B (1987) Solid-state NMR evidence of 4-, 5-, and 6-fold aluminum sites in roller-quenched SiO_2-Al_2O_3 glasses. J Am Ceram Soc 70:C10–C12

Ryerson FJ (1985) Oxide solution mechanisms in silicate melts: systematic variations in the activity coefficient of SiO_2. Geochim Cosmochim Acta 49:637–649

Ryerson FJ, Hess PC (1980) The role of P_2O_5 in silicate melts. Geochim Cosmochim Acta 44:611–624

Ryerson FJ, Hess PC (1978) Implications of liquid-liquid distribution coefficients to mineral-liquid partitioning. Geochim Cosmochim Acta 42:921–932

Sack RO, Carmichael ISE, Rivers M, Ghiorso MS (1981) Ferric-ferrous equilibria in natural silicate liquids at 1 bar. Contrib Mineral Petrol 75:369–376

Skoog DA, West DM (1982) Fundamentals of analytical chemistry. CBS College Publishing, New York, pp 39–90

Tallant DR, Nelson C (1986) Raman investigation of glass structures in the Na_2O-SiO_2-P_2O_5-Al_2O_3 system. Phys Chem Glasses 27:75–79

Thornber CR, Roeder PL, Foster JR (1980) The effect of composition on the ferric-ferrous ratio in basaltic liquids at atmospheric pressure. Geochim Cosmochim Acta 44:525–532

Visser W, Koster van Gross AF (1979) Effects of P_2O_5 and TiO_2 on liquid immiscibility in the system K_2O-FeO-Al_2O_3-SiO_2. Am J Sci 279:970–989

Watson EB (1976) Two-liquid partition coefficients: experimental data and geochemical implications. Contrib Mineral Petrol 56:119–134

Watson EB (1979a) Apatite saturation in basic to intermediate magmas. Geophys Res Lett 6:937–940

Watson EB (1979b) Zircon saturation in felsic liquids: experimental data and applications to trace element geochemistry. Contrib Mineral Petrol 70:407–419

Watson EB, Capobianco CJ (1981) Phosphorus and the rare earth elements in felsic magmas: an assessment of the role of apatite. Geochim Cosmochim Acta 45:2349–2358

Waychunas GA, Brown GE, Ponader CW, Jackson WE (1988) Evidence from X-ray absorption for network-forming Fe^{+2} in molten alkali silicates. Nature 332:251–253

Wells AF (1984) Structural inorganic chemistry. Clarendon Press, Oxford, UK

White AJR, Chappell BW (1988) Some supracrustal (S-type) granites of the Lachlan Fold Belt. Trans R Soc Edinburgh: Earth Sci 73:169-181

Editorial responsibility: T. Grove